Article

Discovery Medicine 2024; 36(184): 1020–1029
https://doi.org/10.24976/Discov.Med.202436184.95

UNC93B1 Mediates the Effects of cGAS-STING on ER Stress and Iron Death, and Reduces Renal Toxicity in Cadmium-Exposed Rats

Renhong Liu[1], Liya Liu[2], Chan Fan[2], Yu Li[2], Yueming Huang[2], Zongwei Yi[2,*]

[1]Department of Neurosurgery, Hunan University of Medicine General Hospital, 418000 Huaihua, Hunan, China
[2]School of Public Health and Laboratory Medicine, Hunan University of Medicine, 418000 Huaihua, Hunan, China
*Correspondence: 15869922088@163.com (Zongwei Yi)
Published: 20 May 2024

Background: Long-term exposure to cadmium can induce renal toxicity in rats, leading to endoplasmic reticulum (ER) stress and iron death. Notably, in cadmium-exposed rats, there is an increased expression of UNC93B1 (unc-93 homolog B1). Consequently, our investigation aims to determine the impact of UNC93B1 on ER stress and iron death in cadmium-exposed rats by modulating the cGAS-STING (cyclic GMP-AMP synthase-stimulator of interferon genes) pathway.

Methods: A cadmium-exposed rat model was established by intrabacally injecting chromium chloride (5 mg/kg, once a day for 4 weeks), and the levels of UCd (urine cadmium), UNAG (urine *N*-acetyl-β-D-glucosaminidase), and UCr (urine creatinine) in urine were assessed. A silent UNC93B1 lentivirus was constructed, and STING agonists were procured and administered to the rats. Subsequently, kidney tissues were extracted post-mortem, and pathological changes in renal tissue were observed through hematoxylin and eosin (HE) staining. The expression and mRNA levels of UNC93B1, cGAS, and STING were examined using western blot (WB) and polymerase chain reaction (PCR). Autophagy proteins (light chain 3 (LC3), Beclin-1, p62) were also assessed by WB. Additionally, iron concentration was determined using a kit, while oxidative stress markers (cytochrome oxidase subunit 2 (COX2), glutathione peroxidase 4 (GPX4), superoxide dismutase (SOD), malondialdehyde (MDA), glutathione (GSH)) were measured through enzyme-linked immunosorbent assay (ELISA). Furthermore, endoplasmic reticulum stress proteins (protein kinase RNA-like ER kinase (PERK), CCAAT enhance-binding protein homologous protein (CHOP), activating transcription factor-4 (ATF4)) were analyzed by WB.

Results: Wstaining, WB, reverse transcription-quantitative polymerase chain reaction (RT-qPCR), ELISA, and HE staining collectively revealed a heightened expression of UNC93B1, cGAS, and STING, accompanied by increased levels of autophagy, oxidative stress, and ER stress in cadmium-exposed rats ($p < 0.05$). Nephrotoxicity exhibited a reduction following the inhibition of UNC93B1, leading to decreased levels of oxidative stress, autophagy, and ER stress ($p < 0.05$). Notably, this observed phenomenon was reversed upon the addition of STING agonists, suggesting that UNC93B1 might exert a nephroprotective effect in cadmium-exposed rats through modulation of the cGAS-STING pathway.

Conclusions: The inhibition of UNC93B1 mitigates nephrotoxicity in cadmium-exposed rats, and this protective effect is mechanistically linked to the cGAS-STING pathway.

Keywords: cadmium exposure; iron death; endoplasmic reticulum stress; cGAS-STING; UNC93B1

Introduction

Cadmium, a pervasive environmental hazard, has been demonstrated to be linked to kidney damage and toxicity [1]. Despite this, the precise mechanisms underlying cellular stress and toxicity resulting from cadmium exposure remain elusive. Recent investigations propose that endoplasmic reticulum (ER) stress and iron death could be pivotal in mediating cadmium toxicity [2]. Endoplasmic reticulum stress, an integral component of cellular stress responses [3], is implicated in the pathogenesis of various diseases, and studies indicate that cadmium exposure induces heightened endoplasmic reticulum stress [4].

In this context, the cGAS-STING (cyclic GMP-AMP synthase-stimulator of interferon genes) signaling pathway has garnered significant attention due to its perceived pivotal role in cellular endoplasmic reticulum stress [5]. UNC93B1 (unc-93 homolog B1), identified as a crucial regulator of the cGAS-STING signaling pathway [6], is postulated to serve as a key nexus linking endoplasmic reticulum stress and toxic effects [7]. While mediating the cGAS-STING signaling pathway, UNC93B1 may also modulate mechanisms associated with iron death [8]. Iron death, considered a novel form of cell demise [9], is believed to be induced by cadmium.

Hence, the primary aim of this study was to investigate the role of UNC93B1 in mediating the cGAS-STING signaling pathway, with a specific focus on its impact on renal toxicity induced by cadmium exposure, particularly within the context of ER stress and iron death. Our goal is to uncover the mechanisms of UNC93B1 in this process, aiming to contribute a new theoretical foundation and potential therapeutic strategies for mitigating kidney injury associated with cadmium exposure.

Methods

Animal Data

We procured 25 male Sprague-Dawley (SD) rats of specific pathogen-free (SPF) grade, weighing 180–220 g and aged 6–8 weeks, from Hunan Slack Jingda Laboratory Animal Co., LTD. (Changsha, China). The animals held an animal production license number: SCKX (Hunan) 2021-0002. Rats were housed in an environment maintained at a temperature of 20–25 °C and a relative humidity of 40–75% and subjected to a 12-hour day/night cycle, with free access to food and water. Prior to the commencement of the experiment, a one-week adaptive feeding period was observed.

All animal experiments received approval from the hospital's Animal Ethics Committee (202102236) and were conducted in strict adherence to the "3R" principle.

Animal Handling and Grouping

Silent UNC93B1 lentivirus (F: 5′-GUAGCUAGCUACGUAGCUA-3′, R: 5′-UAGCUACGUAGCUAGCUAC-3′, PAB13029, Yunzhou Biotechnology Co., LTD.) and a purchased STING agonist (CF501, 2408723-12-4, 5 µg CF501 RBD-Fc formulated for 20 µg) were administered to the rats. The rats were randomly assigned to the following groups: Control, Cd group (model group), Cd+si-NC group (model + blank control group), Cd+si-UNC93B1 group (model + silencing UNC93B1 lentivirus group), Cd+si-UNC93B1+CF501 (model + silencing UNC93B1 lentivirus group + STING agonist group). Each group consisted of five rats, individually housed and fed. Control group rats were injected intrabacally with 0.9% sterile saline of the same volume daily for four consecutive weeks. Cd group rats were instilled with chromium chloride (5 mg/kg, once a day for 4 weeks). The successful establishment of the model was confirmed when UCd (urine cadmium), UNAG (urine *N*-acetyl-β-D-glucosaminidase) and UCr (urine creatinine) levels significantly increased. Other groups received additional treatments based on the Cd group, including si-NC, si-UNC93B1 lentvirus and CF50. Rats in all groups had unrestricted access to water and were not constrained in their activities.

Twenty-four-hour urine samples were collected at 0, 1, 3, 5, 7, 14, 21, and 28 days. Serum and kidney tissues were extracted after rats were anesthetized with 3% sodium pentobarbital and subsequently euthanized.

Biochemical Detection

Serum levels of UCd (urinary cadmium), UNAG (urine *N*-acetyl-β-D-glucosaminidase), and UCr (urinary creatinine) were assessed using an automatic biochemical analyzer.

Hematoxylin and Eosin (HE) Staining

After fixing the kidney tissue in a 10% formaldehyde solution, it underwent a gradient dehydration process before being cryosectioned. Subsequently, the tissue was dewaxed using xylene following further gradient dehydration. Histological changes in the renal tissue were assessed through HE staining.

Western Blot

Tissues were lysed using RIPA buffer enriched with a protease inhibitor at a concentration of 1 mg/mL (1:100; Roche, Basel, Switzerland). Protein concentrations were determined using a BCA assay kit (P0010, Beyotime, Shanghai, China). Subsequently, total proteins from each sample were heated to 95 °C for 10 minutes, electrophoresed on a 10% SDS gel, and then transferred onto a PVDF membrane, which was blocked with 5% non-fat milk. Primary antibodies (1:1000; Rabbit; Abcam, Cambridge, MA, USA) targeting UNC93B1, cGAS, STING, LC3 (light chain 3), Beclin-1, p62, COX2 (cytochrome oxidase subunit 2), GPX4 (glutathione peroxidase 4), SOD (superoxide dismutase), MDA (malondialdehyde), GSH (glutathione), PERK (protein kinase RNA-like ER kinase), CHOP (CCAAT enhance-binding protein homologous protein), ATF4 (activating transcription factor-4) were applied, along with glyceraldehyde-3-phosphate dehydrogenase (GAPDH) (1:1000; Rat; Protein, Inc., Chicago, IL, USA). Subsequent to primary antibody incubation, a horseradish peroxidase (HRP)-linked secondary antibody specific for rabbit/mouse (1:10,000; Jackson Immunology Research, West Grove, PA, USA) was applied. The resulting chemiluminescence was captured using the Bio-Rad ChemDoc system (Hercules, CA, USA) and amplified using enhanced chemiluminescence reagents (Thermo Fisher Scientific, Waltham, MA, USA). Band intensities were quantified using ImageJ software (V1.8.0.112, NIH, Madison, WI, USA).

Quantitative Real-Time PCR

Total RNA was extracted from tissues using the RNA rapid purification kit (Yishan Biotechnology, Shanghai, China). Subsequently, this RNA was reverse-transcribed using the PrimeScript RT kit (RR037A, TaKaRa, Dalian, China) following the provided guidelines. The quantitative polymerase chain reaction (qPCR) analysis was performed with the SYBR Green PCR Master Mix (1725260, Bio-Rad, California, CA, USA). Relative mRNA levels of the tar-

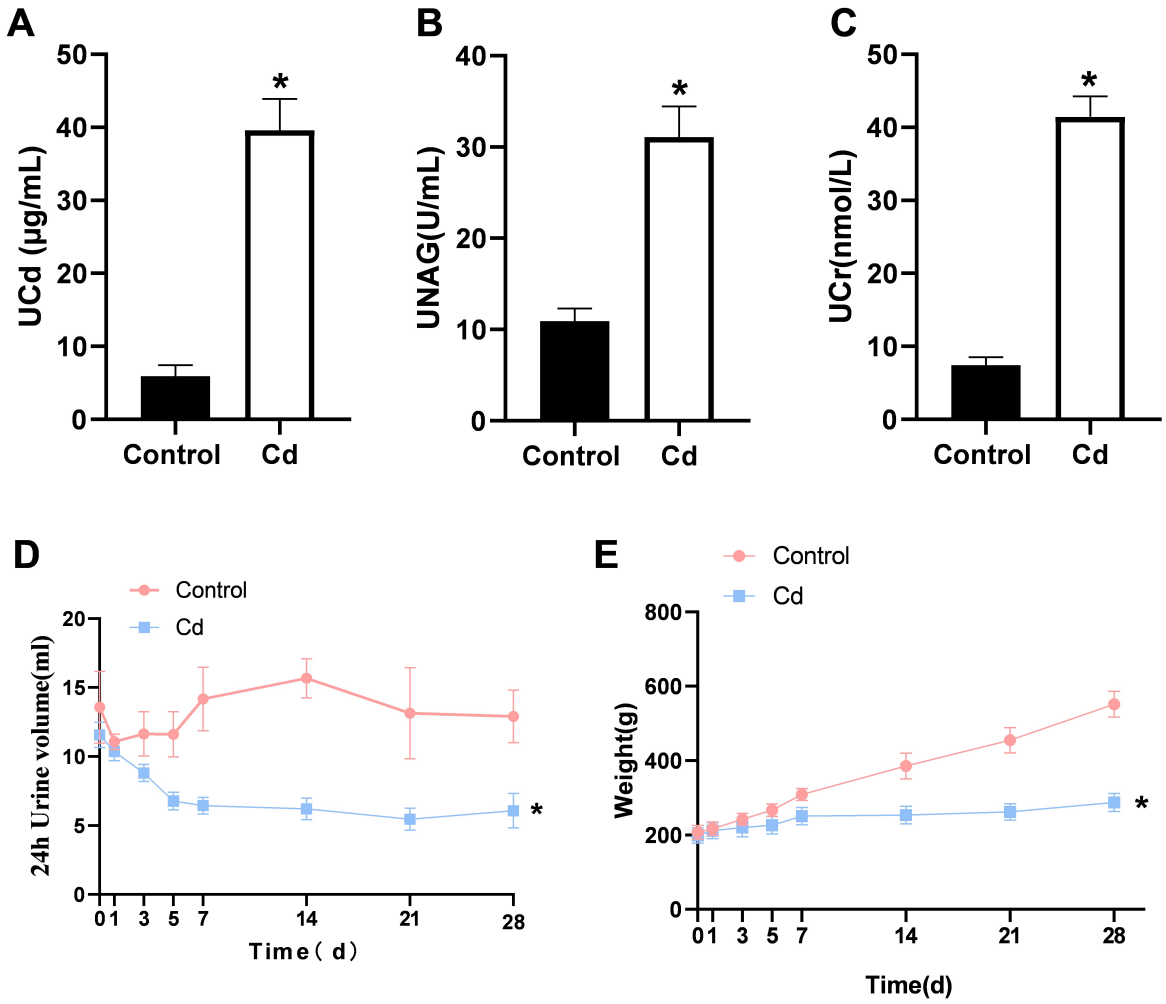

Fig. 1. Establishment of cadmium-exposed rat model. (A–C) For urine cadmium (UCd), UNAG (urine *N*-acetyl-*β*-D-glucosaminidase) and UCr (urine creatinine). (D) Statistics of the urine output in rats. (E) Statistics of urine output of rat body weight. n = 5. *$p < 0.05$ versus Control group.

Table 1. Primers sequence.

Gene	Direction	Sequence (5′-3′)
UNC93B1	F	ATGCGGTAACGTAGTCGGAT
	R	TCGATGGTCCATAGTCGTAG
cGAS	F	ATGGCCTGAGGGTGGGAGTT
	R	TTACTCCAGCCGCTCCACAA
STING	F	ATGGCTGAACTTCTGCAAGGG
	R	TTAGGCAGAGGAAGCGGTCA
β-actin	F	AGAGCTACGAGCTGCCTGAC
	R	AGCACTGTGTTGGCGTACAG

UNC93B1, unc-93 homolog B1; *cGAS*, cyclic GMP-AMP synthase; *STING*, stimulator of interferon genes.

get were determined by normalization against the internal control (*β*-actin) using the $2^{-\Delta\Delta CT}$ method. The specific primers utilized in this study are detailed in Table 1.

Iron Assay

For the determination of iron concentration in tissues, we employed an Iron Assay Kit (MAK025-1KT) following established protocols from prior studies. Tissue samples were rapidly homogenized in 6 volumes of Iron Assay buffer using a homogenizer. The resulting homogenate underwent centrifugation at 16,000 ×g for 10 minutes at 4 °C to eliminate insoluble materials. Subsequently, 50 µL of sample and 50 µL of detection buffer were added to a 96-well plate, and 5 µL of iron assay buffer or iron reducing agent was introduced to each well for ferrous or total iron measurement. Following thorough mixing, the mixture was incubated at 25 °C in the dark. After 30 minutes, 100 µL of Iron Probe was added to each well, followed by another incubation at 25 °C in the dark. After 60 minutes, the 96-well plate was placed in the microplate reader, and absorbance was measured at 593 nm. The iron concentration was calculated using a standard curve.

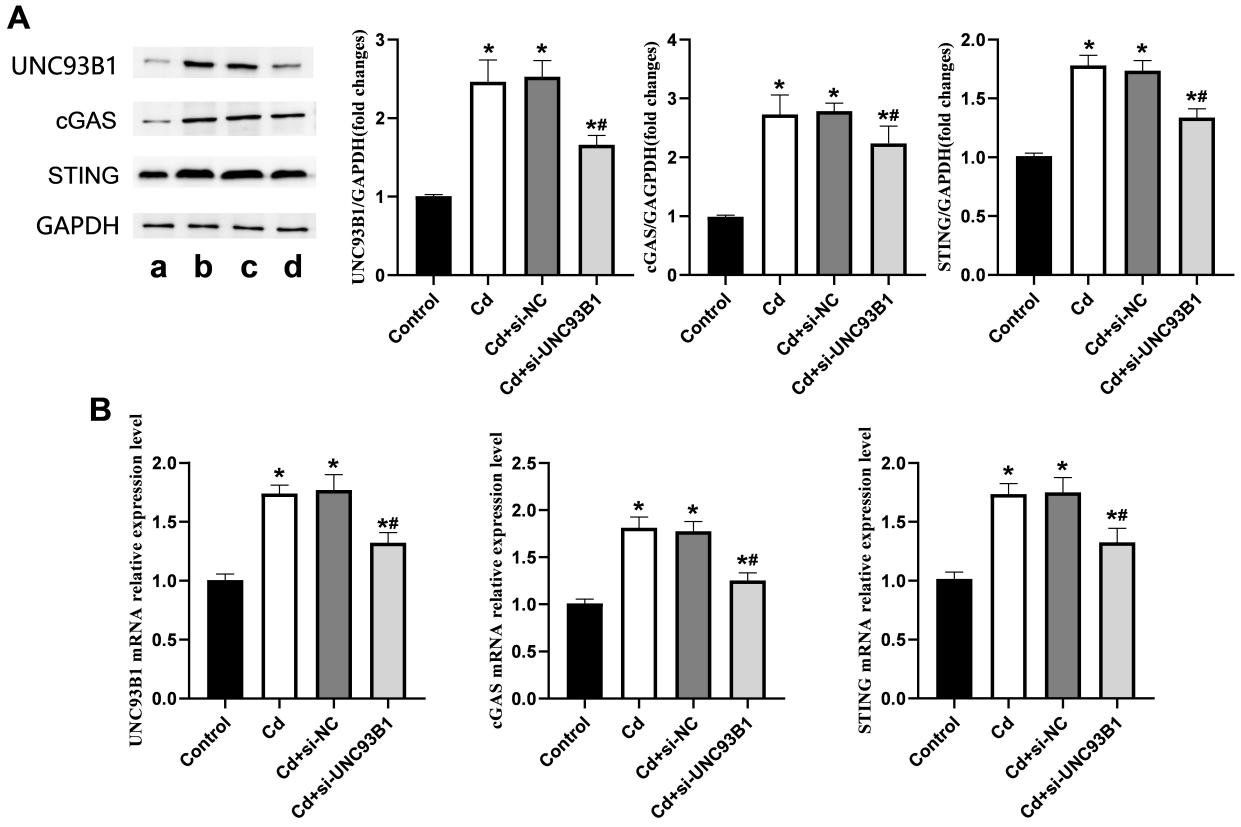

Fig. 2. Effect of UNC93B1 silencing on cGAS-STING (cyclic GMP-AMP synthase-stimulator of interferon genes) expression. (A) The proteins of UNC93B1, cGAS, and STING were detected by western blot (WB). (B) Expression level of UNC93B1, cGAS, and STING mRNA was measured by polymerase chain reaction (PCR). *$p < 0.05$ versus Control group. n = 5. $^{\#}p < 0.05$ versus Cd group. a: group control, b: Cd group, c: Cd+si-NC group, d: Cd+si-UNC93B1 group.

Statistical Analysis

All statistical analyses were conducted using SPSS (IBM, Corp., Armonk, NY, USA) version 24.0, with significance set at $p < 0.05$. Throughout the study, experiments were carried out in triplicate, and results are presented as mean $\pm$ standard deviation ($\bar{\chi} \pm s$). Group comparisons were executed employing one-way ANOVA and *t*-test.

Results

Establishment of Cadmium-Exposed Rat Model

Through the measurement of rat body weight and urine volume, it was observed that both parameters decreased after the modeling process, signifying a significant reduction in both body weight and urine volume ($p < 0.05$). Additionally, the levels of cadmium, UNAG, and UCr in urine were significantly elevated post-modeling ($p < 0.05$) (Fig. 1). This confirms the successful establishment of cadmium-exposed rat models.

Effect of UNC93B1 Silencing on cGAS-STING Expression

The results from western blot (WB) and PCR experiments indicated high expression levels of UNC93B1, cGAS, and STING in both the Cd group and Cd+si-NC group ($p < 0.05$). Following the silencing of UNC93B1 expression, there was a notable decrease in the expressions of cGAS and STING ($p < 0.05$) (Fig. 2). This observation suggests that reducing the expression of UNC93B1 has the potential to inhibit the expression of cGAS-STING.

UNC93B1 Mediates the Effect of cGAS-STING on Histopathology in Cadmium-Exposed Rats

The HE staining results revealed noticeable damage to kidney tissue in both the Cd group and Cd+si-NC group, with evident signs of glomerular bleeding. Interestingly, the Cd+si-UNC93B1 and Cd+si-UNC93B1+CF501 groups showed no significant alteration in the degree of renal tissue injury compared to the Cd group. The inhibition of UNC93B1 and the addition of the STING agonist did not exhibit a substantial improvement in renal tissue injury. These findings confirm the severe damage inflicted by cad-

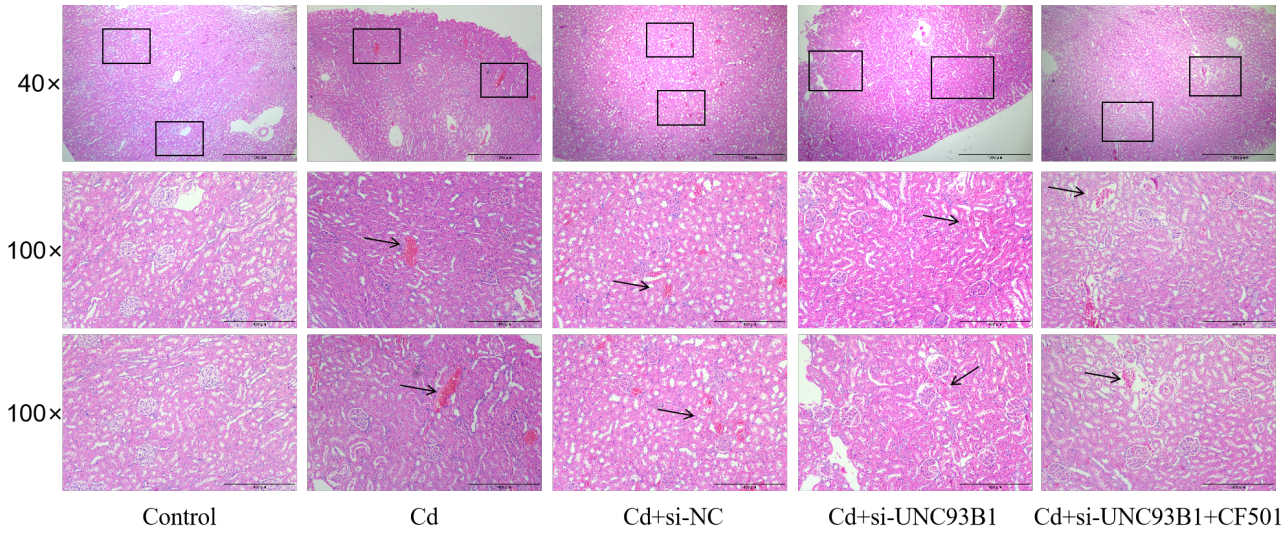

Fig. 3. Hematoxylin and eosin (HE) was stained for cadmium-exposed rat kidney tissue. n = 5. The arrow indicates the site of injury. Scale bars are 1,000 μm and 400 μm, respectively.

mium exposure on rat renal tissue, characterized by significant glomerular hemorrhage and structural disorder. While the inhibition of UNC93B1 had some impact on renal tissue injury, it failed to significantly ameliorate the extent of damage (Fig. 3). This suggests that UNC93B1 might be just one of many influencing factors in the mechanism of kidney injury induced by cadmium exposure, and renal tissue injury could be influenced by a more intricate regulatory network.

UNC93B1 Mediates the Effect of cGAS-STING on Autophagy in Cadmium-Exposed Rats

WB results demonstrated an increase in the expressions of autophagy proteins LC3 and Beclin-1 in both the Cd group and Cd+si-NC group, accompanied by a decrease in the expression of p62 ($p < 0.05$). Following the silencing of UNC93B1, expressions of LC3 and Beclin-1 decreased, and p62 expressions increased compared to the Cd group ($p < 0.05$). Conversely, after the addition of CF501, expressions of LC3 and Beclin-1 increased, and p62 expressions decreased compared to the Cd+si-UNC93B1 group ($p < 0.05$) (Fig. 4). These findings suggest that the inhibition of UNC93B1 could mitigate autophagy, while the addition of CF501 led to an increase in autophagy, aligning more closely with the Cd group.

UNC93B1 Mediates the Effects of cGAS-STING on Iron Death and Oxidative Stress in Cadmium-Exposed Rats

WB results indicated an increase in Fe content, COX2, and MDA expression in both the Cd group and Cd+si-NC group, while GPX4, SOD, and GSH expression decreased ($p < 0.05$). After the silencing of UNC93B1, compared to the Cd group, Fe content, COX2, and MDA expressions decreased, while GPX4, SOD, and GSH expressions increased ($p < 0.05$). However, upon the addition of CF501, compared with the Cd+si-UNC93B1 group, Fe content, COX2, and MDA expressions increased, while GPX4, SOD, and GSH expressions decreased ($p < 0.05$) (Fig. 5). These results suggest that inhibiting UNC93B1 could alleviate iron death and oxidative stress, while adding CF501 increased iron death and oxidative stress, resembling the pattern observed in the Cd group.

UNC93B1 Mediates the Effect of cGAS-STING on Endoplasmic Reticulum Stress in Cadmium-Exposed Rats

WB results demonstrated an increase in the expressions of PERK, CHOP, and ATF4 in both the Cd group and Cd+si-NC group ($p < 0.05$). Following the silencing of UNC93B1, the expressions of PERK, CHOP, and ATF4 decreased compared to the Cd group ($p < 0.05$). Conversely, after the addition of CF501, the expressions of PERK, CHOP, and ATF4 increased compared to the Cd+si-UNC93B1 group ($p < 0.05$) (Fig. 6). These findings suggest that the silencing of UNC93B1 could mitigate ER stress, while the addition of CF501 increased ER stress, aligning with the pattern observed in the Cd group.

Discussion

UNC93B1 plays a crucial role in immune signaling, specifically in the activation of the cGAS-STING pathway [10]. This pathway is essential for detecting DNA virus infections and other sources of intracellular DNA. In the presence of UNC93B1, it facilitates the activation of the cGAS-STING pathway, initiating various immune responses, including the production of interferon and inflammatory factors [11,12]. Recent findings from our research suggest a connection between the activation of the

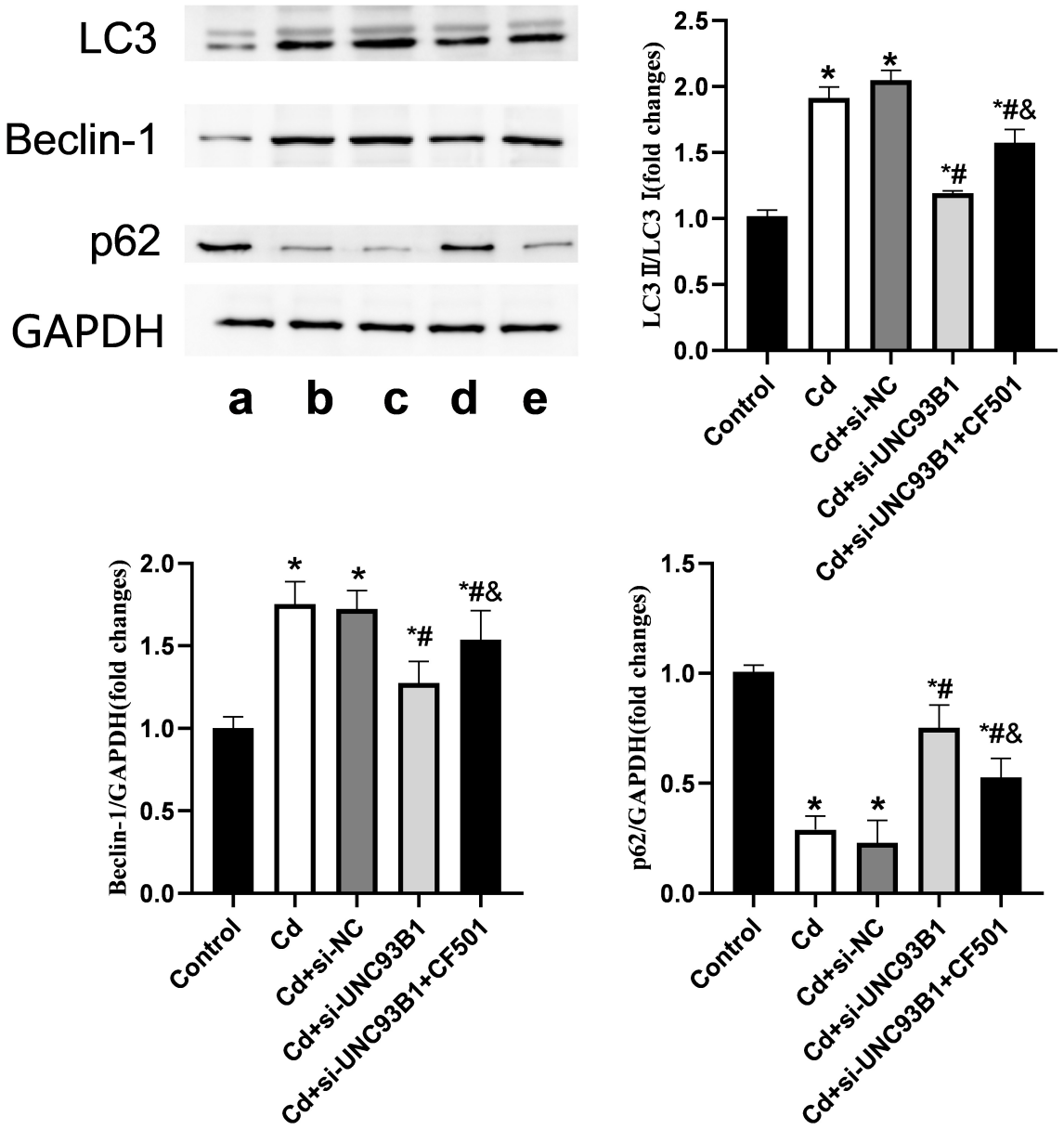

Fig. 4. UNC93B1 mediates the effect of cGAS-STING on autophagy in cadmium-exposed rats. The proteins of light chain 3 (LC3), Beclin-1, and p62 were detected by WB. n = 5. *$p < 0.05$ versus Control group. $^{\#}p < 0.05$ versus Cd group. $^{\&}p < 0.05$ versus Cd+si-UNC93B1 group. GAPDH, glyceraldehyde-3-phosphate dehydrogenase. a: group control, b: Cd group, c: Cd+si-NC group, d: Cd+si-UNC93B1 group; e: Cd+si-UNC93B1+CF501 group.

UNC93B1/cGAS-STING pathway and endoplasmic reticulum (ER) stress. The ER is pivotal in cellular processes, particularly in protein folding and splicing [13]. Activation of the UNC93B1/cGAS-STING pathway may induce ER stress, increasing the demand for protein folding and splicing in the cell, potentially impairing its function.

The activation of the UNC93B1/cGAS-STING pathway also appears to influence iron metabolism in cells [14]. Studies indicate that pathway activation is associated with the occurrence of iron death, a distinct form of cell demise [15], and is associated with the imbalance of iron homeostasis. This effect may be achieved through various mechanisms, including ferritin degradation and the release of iron within the cell [16,17], potentially impacting cell survival. Importantly, this study unveils how UNC93B1 mediates the cGAS-STING pathway to alleviate renal toxicity induced by cadmium exposure. Cadmium, a common toxic metal, poses significant harm to the kidneys [18,19]. The inhibi-

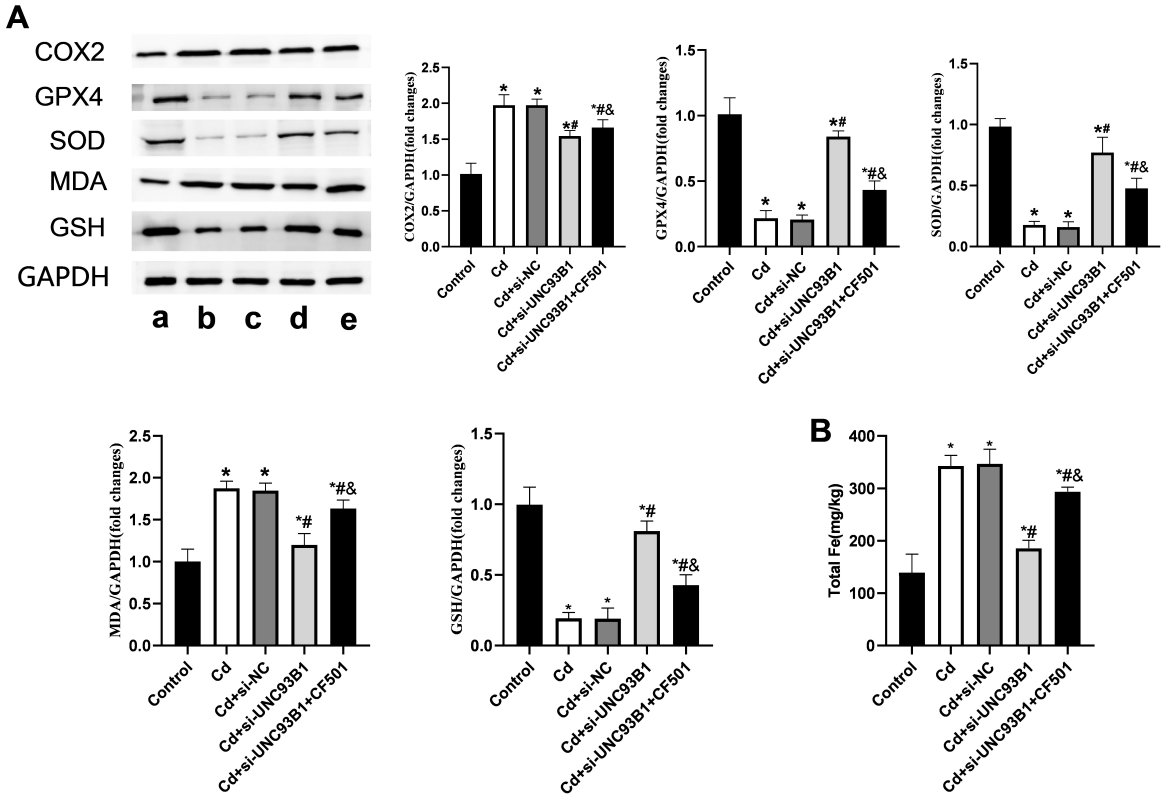

Fig. 5. UNC93B1 mediates the effects of cGAS-STING on iron death and oxidative stress in cadmium-exposed rats. (A) The proteins of cytochrome oxidase subunit 2 (COX2), glutathione peroxidase 4 (GPX4), superoxide dismutase (SOD), malondialdehyde (MDA) and glutathione (GSH) were detected by WB. (B) Kit for total iron content. n = 5. $^{*}p < 0.05$ versus Control group. $^{\#}p < 0.05$ versus Cd group. $^{\&}p < 0.05$ versus Cd+si-UNC93B1 group. a: group control, b: Cd group, c: Cd+si-NC group, d: Cd+si-UNC93B1 group; e: Cd+si-UNC93B1+CF501 group.

tion of UNC93B1 may attenuate kidney damage caused by cadmium exposure by modulating ER stress and iron death [20], offering a novel therapeutic strategy for the prevention and treatment of cadmium poisoning.

The study results indicate that cadmium exposure led to a significant reduction in body weight and urine output, along with a marked increase in urine cadmium, UNAG, and UCr, confirming the successful establishment of a cadmium-exposed rat model. Furthermore, the analysis of UNC93B1, cGAS, and STING expressions revealed a significant increase in these proteins in both the Cd group and the Cd+si-NC group. However, upon inhibiting UNC93B1 expression, the expressions of cGAS and STING were notably reduced, suggesting a regulatory role of UNC93B1 in the cGAS-STING pathway. Additionally, the addition of the STING agonist CF501 led to a re-increase in the expression of cGAS and STING, indicating the regulatory effect of CF501 on the pathway. Moreover, HE staining results illustrated evident renal tissue damage in the Cd group and the Cd+si-NC group, including glomerular hemorrhage and tissue structure disorder.

However, despite inhibiting UNC93B1 expression, kidney tissue was still affected without a significant improvement effect. This suggests that UNC93B1 is just one of many factors contributing to kidney injury induced by cadmium exposure, and renal tissue injury is influenced by a more complex regulatory network. Finally, the WB results also indicated that in the Cd group and Cd+si-NC group, the expressions of autophagy proteins LC3 and Beclin-1 increased, while the expression of p62 decreased, indicating an upregulation in autophagy activity. Autophagy decreased after UNC93B1 inhibition but increased again after the addition of CF501. Additionally, the related indices of oxidative stress and iron death increased in the Cd group and the Cd+si-NC group, while these indices decreased after inhibiting the expression of UNC93B1, suggesting that UNC93B1 plays a regulatory role in iron metabolism and oxidative stress. However, the addition of CF501 led to a resurgence of oxidative stress and iron death. In conclusion, UNC93B1 inhibition of the cGAS-STING pathway reduces autophagy, oxidative stress, ER stress, and iron death, mitigating kidney damage caused by cadmium exposure.

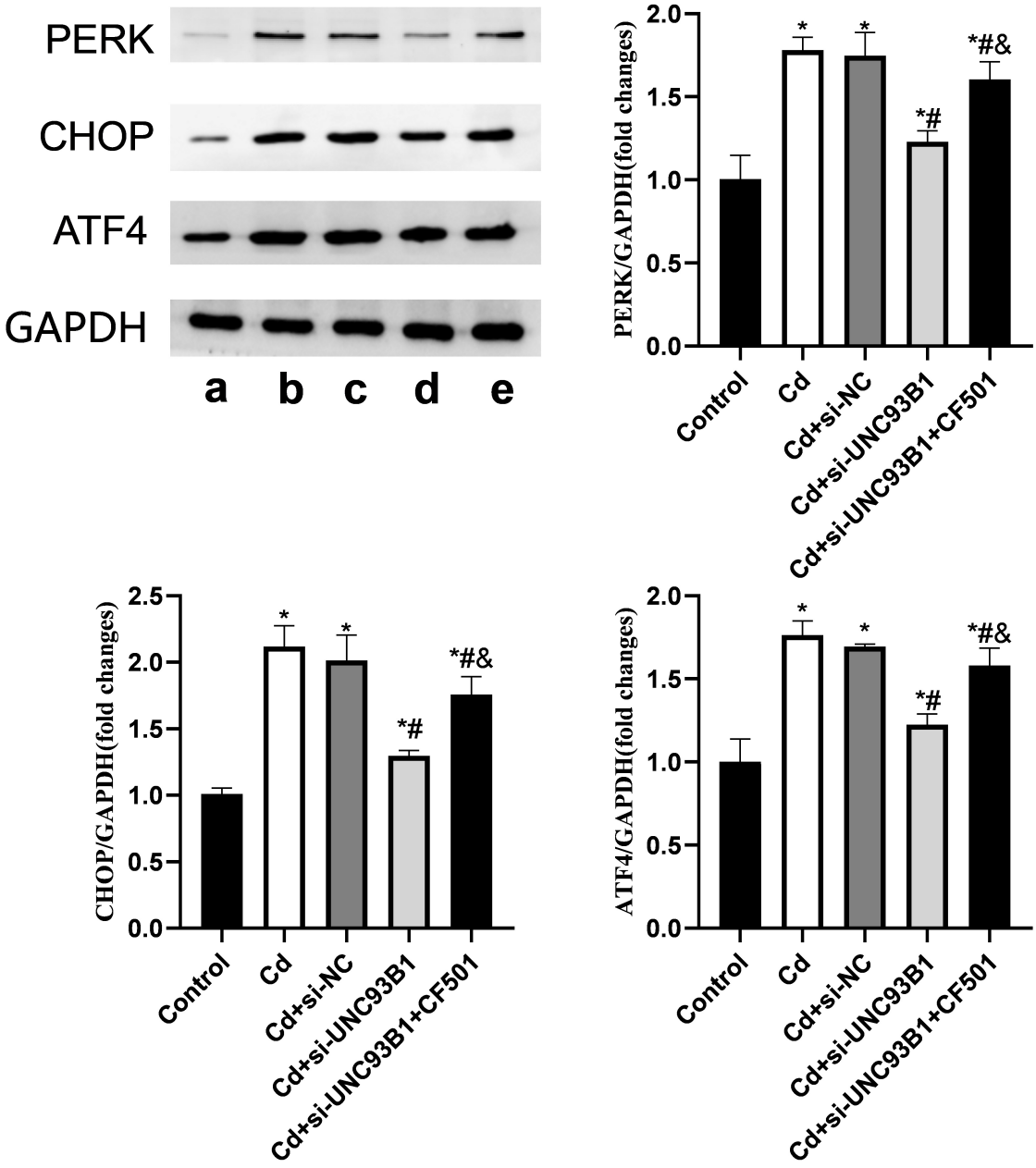

Fig. 6. UNC93B1 mediates the effect of cGAS-STING on endoplasmic reticulum stress in cadmium-exposed rats. The proteins of protein kinase RNA-like ER kinase (PERK), CCAAT enhance-binding protein homologous protein (CHOP) and activating transcription factor-4 (ATF4) were detected by WB. n = 5. $^{*}p < 0.05$ versus Control group. $^{\#}p < 0.05$ versus Cd group. $^{\&}p < 0.05$ versus Cd+si-UNC93B1 group. a: group control, b: Cd group, c: Cd+si-NC group, d: Cd+si-UNC93B1 group; e: Cd+si-UNC93B1+CF501 group.

Our study underscores the pivotal role of UNC93B1 in kidney injury induced by cadmium exposure, specifically in the regulation of the cGAS-STING pathway, autophagy activity, iron metabolism, and oxidative stress. Additionally, our findings suggest that while UNC93B1 is a significant factor, kidney tissue injury is subject to the influence of a complex regulatory network. This sheds new light on the kidney's response to cadmium exposure and offers crucial insights for future intervention and treatment strategies. Our research contributes valuable insights into understanding the mechanism of cadmium toxicity and developing therapeutic approaches for related diseases. It also provides pertinent information for addressing health issues arising from environmental pollution.

In conclusion, our findings suggest that the role of UNC93B1 in kidney injury induced by cadmium exposure is intricate and varied, potentially involving the regulation of multiple pathways, such as autophagy, iron metabolism, oxidative stress, and endoplasmic reticulum stress. It's important to note that the experiments were primarily conducted in a rat model and not on a human basis. Future research should include human-based experiments to further validate the mechanisms of UNC93B1 and the cGAS-STING pathway. Addressing this issue comprehensively requires consideration of multiple factors, and the combined use of STING agonists may offer a potential strategy to alleviate kidney tissue damage.

Conclusions

The inhibition of UNC93B1 has been demonstrated to mitigate nephrotoxicity in cadmium-exposed rats, and this mechanism is associated with the inhibition of the cGAS-STING pathway. Our study results indicate that UNC93B1 inhibition has an impact on nephrotoxicity in cadmium-exposed rats, leading to a reduction in autophagy, iron death, oxidative stress, and endoplasmic reticulum stress.

Availability of Data and Materials

Data used and/or analyzed in the current study are available from the corresponding author upon reasonable request.

Author Contributions

RL, LL and CF designed the research study. LL, CF, YL and YH performed the research. RL, YL and ZY provided help and advice on the experiments. YH and ZY analyzed the data. All authors contributed to editorial changes in the manuscript. All authors read and approved the final manuscript. All authors have participated sufficiently in the work and agreed to be accountable for all aspects of the work.

Ethics Approval and Consent to Participate

The experiment was conducted in strict compliance with the 3R principles and was approved by the animal ethics committee of Hunan University of Medicine General Hospital (202102236).

Acknowledgment

Not applicable.

Funding

It is supported by Hunan Natural Science Foundation Project (2021JJ40388).

Conflict of Interest

The authors declare no conflict of interest.

References

[1] Guo H, Hu R, Huang G, Pu W, Chu X, Xing C, *et al*. Molybdenum and cadmium co-exposure induces endoplasmic reticulum stress-mediated apoptosis by Th1 polarization in Shaoxing duck (Anas platyrhyncha) spleens. Chemosphere. 2022; 298: 134275.

[2] Jia L, Ma T, Lv L, Yu Y, Zhao M, Chen H, *et al*. Endoplasmic reticulum stress mediated by ROS participates in cadmium exposure-induced MC3T3-E1 cell apoptosis. Ecotoxicology and Environmental Safety. 2023; 251: 114517.

[3] Hu W, Xia M, Zhang C, Song B, Xia Z, Guo C, *et al*. Chronic cadmium exposure induces epithelial mesenchymal transition in prostate cancer cells through a TGF-β-independent, endoplasmic reticulum stress induced pathway. Toxicology Letters. 2021; 353: 107–117.

[4] Ge Z, Diao H, Ji X, Liu Q, Zhang X, Wu Q. Gap junctional intercellular communication and endoplasmic reticulum stress regulate chronic cadmium exposure induced apoptosis in HK-2 cells. Toxicology Letters. 2018; 288: 35–43.

[5] Hao XQ, Kou YQ, Xie XJ, JW, Lv JB, Su J, *et al*. Network pharmacology-based study of the anti-oxidative mechanism of san miao wan in treatment of arthritis. World Journal of Traditional Chinese Medicine. 2022; 8: 100–109.

[6] Li JR, Ou YC, Wu CC, Wang JD, Lin SY, Wang YY, *et al*. Endoplasmic reticulum stress and autophagy contributed to cadmium nephrotoxicity in HK-2 cells and Sprague-Dawley rats. Food and Chemical Toxicology. 2020; 146: 111828.

[7] Zeng L, Zhou J, Wang X, Zhang Y, Wang M, Su P. Cadmium attenuates testosterone synthesis by promoting ferroptosis and blocking autophagosome-lysosome fusion. Free Radical Biology & Medicine. 2021; 176: 176–188.

[8] Hong H, Lin X, Xu Y, Tong T, Zhang J, He H, *et al*. Cadmium induces ferroptosis mediated inflammation by activating Gpx4/Ager/p65 axis in pancreatic β-cells. The Science of the Total Environment. 2022; 849: 157819.

[9] Zhou J, Zeng L, Zhang Y, Wang M, Li Y, Jia Y, *et al*. Cadmium exposure induces pyroptosis in testicular tissue by increasing oxidative stress and activating the AIM2 inflammasome pathway. The Science of the Total Environment. 2022; 847: 157500.

[10] Chen X, Bi M, Yang J, Cai J, Zhang H, Zhu Y, *et al*. Cadmium exposure triggers oxidative stress, necroptosis, Th1/Th2 imbalance and promotes inflammation through the TNF-α/NF-κB pathway in swine small intestine. Journal of Hazardous Materials. 2022; 421: 126704.

[11] Yovitania V, Fu QH, Pei J, Zhou H. Neuroprotective effect of electroacupuncture against acute ischemic stroke via PI3K-Akt-mTOR pathway-mediated autophagy. World Journal of Traditional Chinese Medicine. 2022; 8: 339–349.

[12] Wang J, Wang K, Ding L, Zhao P, Zhang C, Wang H, *et al*. Alleviating effect of quercetin on cadmium-induced oxidative damage and apoptosis by activating the Nrf2-keap1 pathway in BRL-3A cells. Frontiers in Pharmacology. 2022; 13: 969892.

[13] Aschner M, Skalny AV, Martins AC, Sinitskii AI, Farina M, Lu R, *et al*. Ferroptosis as a mechanism of non-ferrous metal toxicity. Archives of Toxicology. 2022; 96: 2391–2417.

[14] Yao Y, Zhao X, Zheng S, Wang S, Liu H, Xu S. Subacute cadmium exposure promotes M1 macrophage polarization through oxidative stress-evoked inflammatory response and induces porcine adrenal fibrosis. Toxicology. 2021; 461: 152899.

[15] Tubsakul A, Sangartit W, Pakdeechote P, Kukongviriyapan V, Apaijit K, Kukongviriyapan U. Curcumin Mitigates Hyperten-

sion, Endothelial Dysfunction and Oxidative Stress in Rats with Chronic Exposure to Lead and Cadmium. The Tohoku Journal of Experimental Medicine. 2021; 253: 69–76.

[16] Tong X, Yu G, Liu Q, Zhang X, Bian J, Liu Z, *et al*. Puerarin alleviates cadmium-induced oxidative damage to bone by reducing autophagy in rats. Environmental Toxicology. 2022; 37: 720–729.

[17] Rahmani Talatappeh N, Ranji N, Beigi Harchegani A. The effect of N-acetyl cysteine on oxidative stress and apoptosis in the liver tissue of rats exposed to cadmium. Archives of Environmental & Occupational Health. 2021; 76: 518–525.

[18] Cheng CH, Ma HL, Deng YQ, Feng J, Jie YK, Guo ZX. Oxidative stress, cell cycle arrest, DNA damage and apoptosis in the mud crab (Scylla paramamosain) induced by cadmium exposure. Chemosphere. 2021; 263: 128277.

[19] Hu W, Zhu QL, Zheng JL, Wen ZY. Cadmium induced oxidative stress, endoplasmic reticulum (ER) stress and apoptosis with compensative responses towards the up-regulation of ribosome, protein processing in the ER, and protein export pathways in the liver of zebrafish. Aquatic Toxicology. 2022; 242: 106023.

[20] Mumtaz F, Albeltagy RS, Diab MSM, Abdel Moneim AE, El-Habit OH. Exposure to arsenite and cadmium induces organotoxicity and miRNAs deregulation in male rats. Environmental Science and Pollution Research International. 2020; 27: 17184–17193.